Colorimetric approach towards detection of heavy metal ions by gold nanorods

A

Dissertation

Submitted in partial fulfilment of the requirement for the

Degree of

Masters of Science

In

Chemistry

By

Akanksha Katoch

Roll No.:301702003

Under the Supervision of

Dr. Mily Bhattacharya

(Assistant Professor)

School of Chemistry & Biochemistry
Thapar Institute of Engineering & Technology
Patiala-147004, India

15 July 2019

CERTIFICATE

This is to certify that the dissertation entitled, **"Colorimetric approach towards detection of heavy metal ions by gold nanorods"**, being submitted by **Ms. Akanksha Katoch** in partial fulfilment of requirement for the award of the degree of **Masters of Science** in **Chemistry** and being submitted to the School of Chemistry and Biochemistry, Thapar Institute of Engineering and Technology, Patiala is a bonafide work carried out by her under my supervision. The work has reached the standard necessary for submission, and the contents of this dissertation have not been submitted to any other university or institute for the award of any degree or diploma.

MB 13/8/2019

Dr. Mily Bhattacharya
Assistant Professor
School of Chemistry and Biochemistry
Thapar Institute of Engineering and Technology, Patiala - 147004

CANDIDATE'S DECALARATION

I, hereby, declare that the work being presented in the dissertation entitled **"Colorimetric approach towards detection of heavy metal ions by gold nanorods"** in partial fulfilment of the requirement for the award of the degree of **Masters of Science** in Chemistry and being submitted to School of Chemistry and Biochemistry, Thapar Institute of Engineering and Technology, Patiala is my own research work carried out during the period of January to July 2019 under the supervision of **Dr. Mily Bhattacharya**. I have not submitted the contents embodied in this dissertation for the award of any degree elsewhere.

Akanksha Katoch

Date: Aug 13|2019

It is certified that the above statement made by the student is correct to the best of my knowledge and belief.

13|08|2019

Dr. Mily Bhattacharya
Assistant Professor
School of Chemistry and Biochemistry
Thapar Institute of Engineering and Technology, Patiala – 147004

ACKNOWLEDGEMENT

I would like to avail the opportunity to express my most sincere appreciation and deep gratitude to all those people who in a way or other have contributed positively in the completion of this dissertation. First and foremost, I would like to thank God for giving me strength, knowledge, ability and opportunity to undertake this study and to preserve complete it satisfactorily.

In my journey towards the degree, I express my sincere regards to my supervisor "**Dr Mily Bhattacharya**", Assistant professor, School of Chemistry and Biochemistry, T.I.E.T for inspiring guidance, valuable suggestions and constant encouragement throughout my work. I am grateful for the experience and diverse opportunity given to me while working with her. Her timely approach and discussions have proved greatly valuable in systematic completion of this work. The knowledge, skills and thoughtfulness that she has imparted will be cherished forever.

I am thankful to the Head of the Department "**Dr Amjad Ali**", Associate Professor, School of Chemistry and Biochemistry, for giving me this golden opportunity to carry out my master research and his support during my experiment and allowing me to use UV-Vis spectroscopy. I am thankful to "**Dr. Kamaldeep Paul**", Associates Professor, for being our coordinate and also for his support throughout this entire M.Sc dissertation. I would like to thank "**Dr. Diptiman Choudhury and Dr. Vikas Tiyagi**", for giving me permission to use lab facilities.

I pay huge and warm thanks to all the faculty members who are being understanding and supportive. It' my fortune to gratefully acknowledge all the Ph. D scholars **Ms Jaspreet Kaur, Ms Parmandeep Kaur, Ms Aabida**. They payed a great contribution for successful completion of this M.Sc project. I would like to thank SCBC staff.

This acknowledgment is not completed without my friends, **Anjali Giri**, my lab mate who was always there and motivated me. My best friend **Jemini Dogra**, there always for my help emotionally also. I would thank to my all batch mates with whom I had enjoyed and have fun and had beautiful experience of my life.

I would like to pay high regards to my parents and my sister who have always supported, assisted and encouraged me in achieving my goals.

Akanksha Katoch

ABSTRACT

Gold nanorods (GNRs) have emerged as novel chemosensors and biosensors owing to their excellent optical properties in the visible region. GNRs exhibit two plasmonic bands namely, the longitudinal and transverse surface plasmon resonance bands in the visible region whereby the former can be modulated upon addition of analytes which trigger a change in the aspect ratio of the nanorods. Consequently, the gold nanorods are used for the non-aggregation based colorimetric detection of heavy metal ions such as Cr (VI), Pb (II), Hg (II), etc. In order to investigate the effect of gold nanorods size during interaction with heavy metal ions, two different sizes of gold nanorods *viz.* (GNR (B) and GNR (E)) were synthesized by seed mediated growth mechanism and the changes in the longitudinal absorbance were monitored. CTAB capped seed is used instead of citrate capped seed to get rod shaped particles in the large fraction. For the desired length of gold nanorods, different silver ion content in the growth solution was used. Upon increasing the concentration of silver ions, the aspect ratio (length/width) of gold nanorods increased due to the under potential deposition (UPD). Additionally, the shift in the surface plasmon resonance (SPR) band was observed due to the changes in the concentration of cetyltrimethylammonium bromide (CTAB), aqueous solutions of heavy metal ions, and variable concentration of silver ions. Our findings revealed that the length of gold nanorods shorten significantly due to the redox etching of gold nanorods by Cr (VI) compared to that of Hg (II) and the effect was more prominent for longer GNR(E) compared to the shorter GNR(B). A linear relationship is shown by the blue shift of longitudinal surface plasmon resonance absorption (LSPA) with concentration of Cr (VI).

TABLE OF CONTENTS

	TITLE	PAGE NO.
	ABSTRACT	
CHAPTER 1	**INTRODUCTION**	**1-3**
CHAPTER 2	**LITERATURE REVIEW**	**4-6**
CHAPTER 3	**MATERIALS AND METHODS**	**7**
3.1	Materials	**7**
	3.1.1 Chemical used	7
	3.1.2 Chemical and glassware required	**7**
3.2	Equipment and instrument used	**7**
	3.2.1 Magnetic stirrer with hot plate	**7**
	3.2.2 UV-Vis spectrometer	7-8
3.3	Methodologies	8
	3.3.1 Preparation of stock solution	8
	3.3.1.1 Preparation of aqueous solution of Auric Chloride ($HAuCl_4$)	8-9
	3.3.1.2 Preparation of aqueous solution of CTAB (Cetyltrimethylammonium Bromide) ($C_{19}H_{42}BrN$)	9
	3.3.1.3 Preparation of aqueous solution of Sodium Borohydride ($NaBH_4$)	9
	3.3.1.4 Preparation of aqueous solution of Silver Nitrate ($AgNO_3$)	9
	3.3.1.5 Preparation of aqueous solution of Ascorbic Acid ($C_6H_8O_6$)	9

	3.3.1.6 Preparation of HCl solution	10
	3.3.1.7 Preparation of aqueous solutions of heavy metal ions	10
	3.3.1.7.1 Preparation of aqueous solution of Potassium Dichromate ($K_2Cr_2O_7$)	10
	3.3.1.7.2 Preparation of aqueous solution of Mercuric Chloride ($HgCl_2$)	10
3.4	Synthesis of Gold Nanorods	10
	3.4.1. Preparation of seed solution	11
	3.4.2. Preparation of growth solution	11
3.5	GNRs based sensor for heavy metal ions detection	12
	3.5.1 Sensitivity of heavy metal ion detection by GNRs	13
	3.5.2 GNRs based heavy metal ion sensing at variable incubation times	13
	3.5.3 GNRs prepared by variable concentration of CTAB for heavy metal ion sensing	13
CHAPTER 4	**RESULTS & DISCUSSIONS**	
	4.1 Characterization of gold nanorod and their interaction with heavy metal ions by using UV-Visible absorption Spectroscopy	14-22
CHAPTER 5	**CONCLUSIONS**	23
CHAPTER 6	**REFERENCES**	24-25

LIST OF ABBREVATIONS AND SYMBOLS

Abbreviations

AA-2G	2-*O*-α-D-glucopyranosyl-L-ascorbic acid
BDAC	Benzyldimethylhexadecylammonium Chloride
CTAB	Cetyltrimethylammonium Bromide
GNRs/ AuNRs	Gold Nanorods
HRTEM	High Resolution Transition Emission Microscopy
LSPA	Longitudinal Surface Plasmon Absorbance
SPR	Surface Plasmon Resonance
TEM	Transition Emission Microscopy
UV-Visible	Ultraviolet-Visible
UPD	Under Potential Deposition

Symbols and Chemical Formulae

$AgNO_3$	Silver Nitrate
Cr	Chromium
$C_6H_8O_6$	Ascorbic acid
$C_{19}H_{42}BrN$	Cetyltrimethylammonium Bromide
$HgCl_2$	Mercury Chloride
HCl	Hydrochloric acid
$HAuCl_4$	Auric Chloride
KIO_3	Potassium Iodate
$K_2Cr_2O_7$	Potassium Dichromate
$NaBH_4$	Sodium Borohydride
°C	Degree Celsius
μL	Micro litre
μM	Micro molar
nm	Nano meter

LIST OF FIGURES

Figure 1.1: Different shapes of gold nanoparticles.

Figure 1.2: Seed mediated growth mechanism for gold nanorods.

Figure 3.4.1: Schematic diagram for the synthesis of seed solution.

Figure 3.4.2: Gold nanorods synthesized by seed mediated growth mechanism by seed-mediated growth mechanism (a) GNR (B) (b) GNR (E).

Figure 3.4.3: Schematic diagram for the synthesis of GNR growth solution.

Figure 4.1: UV-Vis absorption spectra of CTAB-capped gold nanorods (a) GNR (E) (b) GNR (B).

Figure 4.2: UV-Visible absorption spectra of effect of heavy metal ions on GNR (E) (a) Conc. dependent study of Cr (VI) at 50 °C for 30 min (b) Conc. dependent study of Hg (II) at 50 °C for 30 min.

Figure 4.3: UV-Visible absorption spectra of effect of heavy metal ions on GNR (E) for Cr (VI) at 50 °C for 30 min (a) Sensitivity dependent study of Cr (VI) [2×10^{-4} M] (b) Sensitivity dependent study of Cr (VI) [2×10^{-8} M] (c)Sensitivity dependent study of Cr (VI) from [2×10^{-4} M]- [2×10^{-8} M].

Figure 4.4: UV-Visible absorption spectra of effect of heavy metal ions on GNR (B) (a) Conc. dependent study of Cr (VI) at 50 ℃ for 30 min (b) Conc. dependent study of Hg (II) at 50 ℃ for 30 min.

Figure 4.5: UV-Visible absorption spectra of effect of heavy metal ions on GNR (B) for Cr (VI) at 50 °C for 30 min (a) Sensitivity dependent study of Cr (VI) [2×10^{-4} M] (b) Sensitivity dependent study of Cr (VI) [2×10^{-8} M] (c) Sensitivity dependent study of Cr (VI) from [2×10^{-4} M]- [2×10^{-8} M].

Figure 4.6: UV-Visible absorption spectra of effect of heavy metal ion Cr (VI) [20 μM] (a) Time dependent study for GNR (E) at 50 °C (b) Time dependent study for GNR (B) at 50 °C.

Figure 4.7: UV-Visible absorption spectra of CTAB conc. dependent study (a) For GNR (E) at 50 °C for 30 min (b) For GNR (B) at 50 °C for 30 min.

Figure 4.8: UV-Visible absorption spectra of effect of heavy metal ion Cr (VI) at 50 °C for 30 min (a) CTAB conc. dependent study of Cr (VI) [10 μM] on GNR (E) (b) Effect of CTAB conc. on the Δλ of Cr (VI) [10 μM] on GNR (E) (c) CTAB conc. dependent study of Cr (VI) [20 μM] on GNR (E) (d) Effect of CTAB conc. on the Δλ of Cr (VI) [20 μM] on GNR (E).

Figure 4.9: UV-Visible absorption spectra of effect of heavy metal ion Hg (II)) at 50 °C for 30 min (a) CTAB conc. dependent study of Hg [10 μM] on GNR (E) (b) Effect of CTAB conc. on the Δλ of Hg [10 μM] on GNR (E) (c) CTAB conc. dependent study of Hg [20 μM] on GNR (E) (d) Effect of CTAB conc. on the Δλ of Hg [20 μM] on GNR (E).

Figure 4.10: UV-Visible absorption spectra of effect of heavy metal ion Cr (VI) at 50 °C for 30 min (a) CTAB conc. dependent study of Cr [10 μM] on GNR (B) (b) Effect of CTAB conc. on the Δλ of Cr [10 μM] on GNR (B) (c) CTAB conc. dependent study of Cr [20 μM] on GNR (B) (d) Effect of CTAB conc. on the Δλ of Cr [20 μM] on GNR (B).

Figure 4.11: UV-Visible absorption spectra of effect of heavy metal ion Hg (II) at 50 °C for 30 min (a) CTAB conc. dependent study of Hg [10 μM] on GNR (B) (b) Effect of CTAB conc. on the Δλ of Hg [10 μM] on GNR (B) (c) CTAB conc. dependent study of Hg [20 μM] on GNR (B) (d) Effect of CTAB conc. on the Δλ of Hg [20 μM] on GNR (B).

Figure 4.12: TEM image for GNR (E) + 20 μM of Cr (VI) after 5 days.

CHAPTER 1 INTRODUCTION

Nanotechnology accentuates materials in the scale of 10^{-9} meter, involving medicines, biotechnology, material sciences, biophysical, biomedical carriers [1]. From the Greek word, the term nano was derived which means little or minute. The particles in the size range of 1 – 100 nm and have two or more than two dimensions are called as nanoparticles. Due to the large reactive and exposed surface area, nanoparticles have unique and magnified chemical and physical properties [2]. Gold nanoparticles have different shapes like nanosphere, nanostar, nanorod, nanocluster etc as shown in (Fig. 1.1). Gold nanoparticles studies are revelent to the metallic nano particles, due to the easy preparation, good stability and some unique properties of the gold nanoparticles [3].

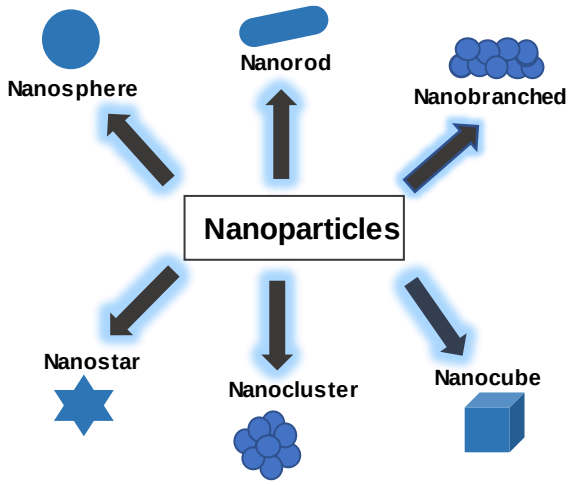

Fig 1.1. Different shapes of gold nanoparticles (Khan *et al.* (2014) [2]).

There is extreme technological interest in gold nanorods (AuNRs) due to their optical properties and widely tunable surface plasmon resonance. Due to the SPR they strongly absorb the light in the visible region [4]. Two plasmon bands have shown splitting into transverse plasmon bands having the shorter wavelength for the gold nanorods, corresponding to light absorption and scattering along the short axis of particle and longitudinal plasmon band having longer wavelength, corresponding to light absorption and scattering along the long axis of particle [5]. The absorption and scattering of electromagnetic radiations are strongly increased by the gold nanorods as the surface of GNRs has strong electric field. The nanoparticles have

applications in the medical diagnosis due to its strong longitudinal surface plasmon resonance [LSPR] extinction as well as high sensitivity [6]. Typically, gold nanorods have wide applications in biological and medical use for the dark field, photothermal therapy for cancer cells, photon luminescence diagnostic imaging and for the drugs delivery they are used as a messenger [7]. Due to these properties gold nanorods have many applications in MRI contrast agents, electron microscopy and optical spectroscopy applications [8].

GNRs show the strong LSPR due to which they act as a colorimetry sensor for the detection of Cr (VI) [9]. For plants, animals, bacteria, Cr (VI) is too much toxic element. It has many carcinogenic effects as well as nerve tissue degrading factors. The contaminated level of Cr (VI) in water should be 100 ppb. Nowdays in many industries Cr (VI) is widely used including pigment fabrication, leather tanning, wood preserving, dyes pigments, chromium plating etc [10]. For the better understanding of interaction of heavy metal ions with gold nanorods, two different size of gold nanorods was used GNR (B) having light purple solution is associated with shift towards the shorter wavelength , which is smaller in size with longitudinal absorption band at 663 nm and GNR (E) having wine red solution is associated with shift towards the longer wavelength (red shift), which is longer in size with longitudinal absorption band at 799 nm. The gold nanorods were synthesized by seed mediated growth mechanism involving chloroauric acid ($HAuCl_4$) and CTAB in the presence of a strong reducing agent [11]. CTAB acts as surfactant as well as capping agent for the gold nanorods. CTAB binds strongly around the gold nanorods, inhibits further growth, and enhances the monodispersity [12]. Many parameters like seed concentration, surfactant concentration, silver concentration, ascorbic acid concentration, pH, temperature affects the size, monodispersity, yield of the gold nanorods. Silver ion has the role to get desire length of the gold nanorods, which restrict the particles growth as the Ag-Br pair adsorption on the various facets of gold nanorods as the shown in (Fig. 1.2) [13]. In this research work, the change in the gold nanorods with heavy metal ions have monitored, both in isolation as well as mixture. In the visible range, gold nanoparticles have strong surface plasmon resonance absorption (SPR) and very high extinction coefficient $10^{-8} – 10^{-10}$ M^{-1} cm^{-1}. Due to coherent electronic oscillations gold nanorods have substantially strong longitudinal plasmon absorption (LPA) and larger extinction coefficient than that of gold nanoparticles. Moreover, LPA is very sensitive and dependent on the gold nanorods length.

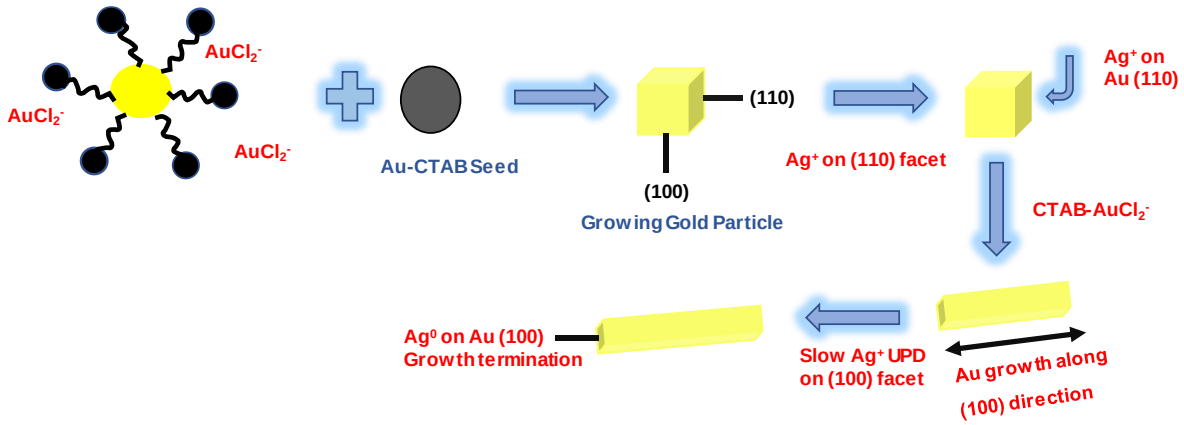

Fig. 1.2. Seed mediated growth mechanism for gold nanorods (Huang *et al.* (2009) [18]).

The blue shift in the longitudinal plasmon absorption (LPA) is due to the etching of gold nanorods by Cr (VI), decreases the aspect ratio (length/width) of gold nanorods. Hence, towards Cr (VI), colorimetric sensors show sensitive, simple and selective response [14]. The optical properties of the gold nanorods were examined by spectroscopic techniques like UV-Vis spectroscopy and TEM.

CHAPTER 2 LITERATURE REVIEW

Nikoobakht and El-Sayed (2003) [11] had reported synthesis of gold nanorods (GNRs) with varying aspect ratios (length/width) in between the range of 1.5 to 10, using both strong reducing agent such as sodium borohydride ($NaBH_4$) and a mild reducing agent such as ascorbic acid which reduced chloroauric acid ($HAuCl_4$). They had used CTAB capped seeds instead of citrate capped seeds to avoid the formation of spherical particles. For the synthesis of GNRs of desired aspect ratios, the silver content in the growth solution was modulated. Additionally, for the synthesis of longer NRs with aspect ratios (length/width) ranging in between 4.6 to 10, they had used a binary surfactant mixture of benzyldimethylhexadecylammonium Chloride (BDAC) and cetyltrimethylammonium Bromide (CTAB). The solution was stirred for 13-14 hr and centrifugation was carried out to remove the spherical particles and assemble the NRs. The synthesized NRs were characterized by UV-Vis spectroscopy and TEM. Gole *et al.* (2004) [15] had reported the synthesis of stable and monodisperse (stabilized by bilayer of CTAB) GNRs by three different seeding protocols. They had studied both positively and negatively charged surface group seeds with the diameter ranging from 4 nm to 18 nm. Seeds were added into the growth solution containing chloroauric acid ($HAuCl_4$), surface directing agent CTAB and a mild reducing agent (ascorbic acid). They had investigated the dependence of nanorods aspect ratios (length/width) on the seed size as well as the charge on the seed. Characterization of the nanorods were carried out using UV-Vis spectroscopy, TEM, Fourier transform infrared spectroscopy. Orendorff *et al.* (2006) [16] had studied the silver assisted growth of GNRs having aspect ratios (length/width) in the range of 2 to 4.5 using sodium borohydride ($NaBH_4$), ascorbic acid and chloroauric acid ($HAuCl_4$). They had prepared the spherical gold particles by boiling chloroauric acid with sodium citrate. Centrifugation was carried out to separate gold nanorods from unnecessary particles. They had reported that a high yield of GNRs were obtained due to the addition of Ag^+ resulting in elongation in length as compared to citrate capped seeds in the absence of Ag^+, since UPD of silver should be faster on the sides of the GNRs [110] facet than on the ends [100] facet, which resist the growth of gold nanorods from sides and enhances the growth of GNRs at the ends. They had characterized the gold nanorods by inductively coupled plasma atomic emission spectroscopy, UV-Vis spectroscopy, and transmission electron microscopy (TEM). Li *et al.* (2011) [9] had studied the synthesis of gold nanorods and their application as non-aggregation

based colorimetric sensor which showed highly selectivity and sensitivity towards Cr (VI) detection. They observed that the GNRs length decreased as the concentration of Cr (VI) increased due to the amplified redox etching of GNRs activated by Cr (VI). Also, they had reported that the selective etching is temperature dependent, and the aspect ratio (length/width) of the GNRs decreased with an increase in the temperature and a corresponding blue-shift was observed by UV-Vis spectroscopy. However, the longitudinal plasmon absorption increased with an increase in the CTAB concentration. Consequently, UV-Vis spectroscopy showed a red shift due to an increase in GNRs aspect ratio (length/width). Cheng *et al.* (2019) [17] had discussed the ultrasensitive colorimetric method for the α-glycosidase activity sensing based on GNRs etching. The GNRs were synthesised using both strong reducing agent namely, sodium borohydride ($NaBH_4$) and mild reducing agent namely, ascorbic acid which caused the reduction of chloroauric acid ($HAuCl_4$). They had used CTAB as surfactant as well as capping agent. GNRs were used for colorimetric sensing system for the α-glycosidase detection based on iodine-mediated GNRs etching. The authors have reported that ascorbic acid reduced KIO_3 to generate I_2, which etched GNRs stabilized by CTAB. They had observed a blue shift of LSPR absorption, which indicated a reduction in the aspect ratio (length/width) of GNRs. Additionally, the activity of α-glycosidase was inhibited as a function of enhanced concentration of acarbose. The aspect ratio of GNRs and the blue shift of LSPR absorption were analysed by TEM and UV-Vis spectrophotometer. Huang *et al.* (2009) [18] had studied properties, applications and synthesis of gold nanorods. They had synthesised high yield GNRs with aspect ratios (length/width) from 1.5 to 4.5. The HRTEM and electron diffraction pattern had demonstrated the presence of pentatetrahedral twinned structure of GNRs with citrate capped seeds in the absence of any silver ions. They had also discussed the potential of GNRs in wide range of biomedical applications such as drug diagnosis, treatment and therapeutic studies. Johnson *et al.* (2002) [19] had discussed the synthesis of gold nanorods via the seed-mediated growth process. The HRTEM and electron diffraction analysis had shown that the symmetric reduction was linked with cyclic penta-twinning of the fcc lattice. It was suggested that the initial growth and aggregation induces breaking of cubic symmetry, which produced isomeric twinned particles with a decahedral morphology when the seed was added. They had also determined the interaction between the headgroups of cationic surfactant and the side facets of growth. Zhang *et al.* (2014) [20] had studied the highly sensitive and selective visual sensing of Cu^{2+} by GNRs, that led to a change in the shape dependent LSPR spectroscopy on the basis of catalytical etching of GNRs. They had mentioned that the GNRs were etched in

the length-wise direction by the addition of Cu^{2+} which resulted in a decrease in the aspect ratio (length/width). UV-Vis spectroscopy and TEM measurement were used to monitor the blue shift of GNRs. They had reported that the etching enhanced as the concentration of CTAB increased, since the etching process was altered by CTA^{+} but not by enhancing the Br^{-} concentration.

CHAPTER 3 MATERIALS AND METHODS

3.1 Materials

3.1.1 Chemicals used

Auric Chloride ($HAuCl_4$), Cetyltrimethylammonium bromide (CTAB; $C_{19}H_{42}BrN$), Sodium Borohydride ($NaBH_4$), Silver Nitrate ($AgNO_3$), Ascorbic Acid ($C_6H_8O_6$), Potassium Dichromate ($K_2Cr_2O_7$), Mercuric Chloride ($HgCl_2$). From Sigma-Aldrich all the chemicals were bought. All the aqueous solution of these chemicals were prepared in ultrapure Milli-Q water (Millipore).

3.1.2 Glassware and Labware required

Micropipettes (2-20 μL, 20-200 μL, 100-1000 μL; Eppendorf Research), micropipette tips, volumetric flask, reagent bottles, glass vials (20 mL), magnetic stir bars, micro-centrifuge tubes (1.5 mL and 2 mL), measuring cylinder, Quartz cuvettes (2.5 mL), spatula, burette, burette stand, kim-wipes.

3.2 Equipment and Instrument used

3.2.1 Magnetic stirrer with hot-plate

In this research work, a magnetic stirrer with hot-plate (IKA RCT Basic) was used. It has a maximum heating temperature up to 310 ℃ and a maximum speed of 1800 rpm. In this research work, the stirring speed was set at 300 rpm and the temperature was set at 30 ℃.

3.2.2 UV-Vis Spectrophotometer

In this research work, UV-Vis spectrophotometer (PerkinElmer Lambda 35) was used. The UV-Vis spectrophotometer is an instrument which is used for the detection transitions between the electronic energy levels of molecules. In electronic excitations the electrons are promoted from ground state to the higher energy excited state upon absorption of photons and these transitions occur in the range of 200 - 800 nm that is manifested as the UV and visible spectrum. It is also known as absorption spectroscopy whereby molecules containing bonding and non-

bonding electrons absorb photons in the form of UV and visible light. Four transitions are possible ($\pi-\pi^*$, $n-\pi^*$, $\sigma-\sigma^*$ and $n-\sigma*$). The Beer-Lambert law is followed during the UV-Vis absorption, which states that when a monochromatic light passes through a solution of an absorbing substance, then the absorbance of the solution is directly proportional to the concentration of the absorbing species in the solution and the path length.

$$\mathbf{A = \log_{10}(I_o/I) = \varepsilon cl}$$

Where A: Absorbance, I_o: Intensity of incident light, I: Intensity of transmitted light, C: molar concentration of solute, l: path length of the cuvette in cm, and ε: molar absorptivity

The UV-Vis spectrophotometer primarily consists of two sources of light: deuterium discharge lamp and tungsten filament lamp. For the UV-region (200 nm – 400 nm), deuterium lamp is used and for the visible region (400 nm – 800 nm), tungsten filament lamp is used. Typically, a double beam UV-Vis spectrophotometer is used in which before reaching the sample, the light is split into two beams. One beam is used as the reference which passes through the solvent that is used for preparing the sample solution whereas the other beam passes through the sample solution. The intensity of reference beam is taken as 100 % transmittance and 0 absorbance. The spectrophotometer consists of two detectors (photodiodes), which measure the absorbance from the sample and the reference simultaneously. Sample solutions are taken in a cuvette (made up of quartz). The cuvette has two opaque faces and two transparent faces. The transparent side of the cuvette containing the sample is placed in front of the lamp. This allows light to get transmitted from the sample and is detected by photodiode. Finally, absorbance is plotted as a function of wavelength. In this research work, following parameters were used for recording the absorbance of the samples; Scan range: 400 nm – 1100 nm, Scan speed: 480 nm/min, Bandwidth: 1 nm and Pathlength: 1 cm.

3.3 Methodologies

3.3.1 Preparation of stock solutions

3.3.1.1 Preparation of aqueous solution of Auric Chloride ($HAuCL_4$)

The Auric Chloride stock solution was prepared in a volumetric flask at a concentration of 50 mM in 50 mL of milli-Q water. The volumetric flask was properly covered with the aluminium

foil after the stock solution of Auric Chloride was prepared and placed at room temperature in the dark, protected from the sunlight to ensure its prolonged stability.

3.3.1.2 Preparation of aqueous solution of CTAB (Cetyltrimethylammonium Bromide) ($C_{19}H_{42}BrN$)

The CTAB stock solution was prepared in a reagent bottle at a concentration of 0.2 M in 50 mL of milli-Q water. Typically, the powered CTAB was weighed (3.64 g) in an analytical balance and dissolved in 50 mL of milli-Q water. In order to get a clear solution without any foam/bubble, the CTAB solution was kept in a water bath at 30 ℃ and gently shaken at times whereby CTAB dissolved gradually. The CTAB stock solution was stored at room temperature and it was freshly prepared every time as and when required.

3.3.1.3 Preparation of aqueous solution of Sodium Borohydride ($NaBH_4$)

The sodium borohydride stock solution was prepared in a glass vial at a concentration of 0.01 M in 12.5 mL of milli-Q water. The free-flowing powered sodium borohydride was weighed (5 mg) in an analytical balance. As sodium borohydride is extremely hygroscopic, it was dissolved quickly in 12.5 mL of ice-cold milli-Q water at room temperature as it reacts exothermically with water to generate flammable hydrogen gas. It was also freshly prepared every time as and when required.

3.3.1.4 Preparation of aqueous solution of Silver Nitrate ($AgNO_3$)

The silver nitrate stock solution was prepared in a glass vial at the concentration of 0.004 M in 10 mL of milli-Q water. The powdered silver nitrate was weighed (6.8 mg) in an analytical balance and dissolved in 10 mL of milli-Q water at room temperature. After dissolving it, the glass vial was covered quickly with aluminium foil as silver nitrate is photosensitive (sensitive to light), it breaks down to give black or brown silver oxide and nitric acid. It was stored at 4 °C in the fridge, was protected from sunlight and freshly prepared every time as and when required.

3.3.1.5 Preparation of aqueous solution of Ascorbic Acid ($C_6H_8O_6$)

The ascorbic acid stock solution was prepared in a glass vial at the concentration of 0.0788 M in 10 mL of milli-Q water. The ascorbic acid was weighed (138.8 mg) in an analytical balance

and dissolved in the 10 mL of milli-Q water at room temperature. It was stored at 4 °C in the fridge, was protected from sunlight and freshly prepared every time as and when required.

3.3.1.6 Preparation of HCl solution

The stock solution of HCl was prepared at a concentration of 1 M in milli-Q water at room temperature. Typically, a sub-stock of HCl was prepared (0.5 M) in order to use it, for our required experiments. A 5 mL aliquot was transferred into 10 mL of milli-Q water.

3.3.1.7 Preparation of aqueous solutions of heavy metal ions

3.3.1.7.1 Preparation of aqueous solution of Potassium Dichromate ($K_2Cr_2O_7$)

The potassium dichromate stock solution was prepared in a glass vial at a concentration of 0.01 M in 20 mL of milli-Q water. The potassium dichromate was weighed (58.8 mg) in an analytical balance and dissolved in 20 mL of milli-Q water at room temperature. The stock solution was stored at room temperature and it was stable for a long period of time.

3.3.1.7.2 Preparation of aqueous solution of Mercuric Chloride ($HgCl_2$)

The mercuric chloride stock solution was prepared in a glass vial at a concentration of 0.01 M in 20 mL of milli-Q water. The mercuric chloride was weighed (54.3 mg) in an analytical balance and dissolved in 20 mL of milli-Q water at room temperature. The stock solution was stored at room temperature used and it was stable for a long period of time.

3.4 Gold Nanorods synthesis

For the GNRs synthesis, each of the glass apparatus was first washed with water, then cleaned with freshly prepared aqua regia, and again washed thoroughly with substantial volumes of milli-Q water and dried in an oven overnight. In this research work two different GNRs were prepared i.e. GNR (B) and GNR (E) using a well-known protocol as described by Nikoobakht *et al.* (2003) [10]. Following is a brief description of the nanorod synthesis procedure which was used in this research work.

3.4.1. Preparation of seed solution:

5 mL of CTAB (0.2 M) was taken in a 20 mL glass vial and 5mL of $HAuCl_4$ (0.00050 M) was mixed into it. The resultant golden colored solution was stirred at a speed of 300 rpm at 30 ℃. In the stirred solution, freshly prepared ice-cold $NaBH_4$ (0.01 M) of 0.60 mL of was added immediately into the stirred solution. $NaBH_4$ is a strong reducing agent which changed the color of the solution from golden to brownish yellow, which shows the creation of gold nano seeds (Fig. 3.4.1). Vigorous stirring of seed solution was done for 2 minutes. Thereafter, seed solution was kept at 30 ℃ with stirring at the speed of 300 rpm for 2 hours.

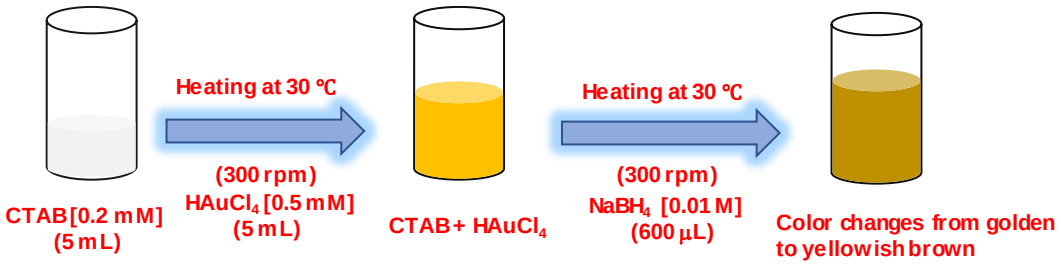

Fig 3.4.1: Schematic diagram for the synthesis of seed solution.

3.4.2. Preparation of growth solution:

5 mL of CTAB (0.2 M) was added to (0.10 mL, 0.25 mL) of $AgNO_3$ (0.0040 M) solution in a 20 mL of glass vial and was stirred at 300 rpm at 30 ℃. The size of GNRs is based on the volume of $AgNO_3$. For example, addition of 0.10 mL of $AgNO_3$ led to the formation of GNR (B), which is smaller in size whereas addition of 0.25 mL of $AgNO_3$ led to the formation of GNR (E), which is larger in size (Fig. 3.4.2). 5 mL of $HAuCl_4$ (0.0010 M) was added to the solution. After mixing the solution gently, 70 µL of Ascorbic acid (0.0788 M) was mixed to the solution. Ascorbic acid acts as a mild reducing agent which led to the formation of colorless solution from the golden solution (Fig. 3.4.3). Now 12 µL of freshly prepared seed solution was added to the growth solution all at once. The change in the solution color was examined within 10-20 min. Stirring of the solution was done for 2 hours at 30 ℃. The solution of GNRs was centrifuged at 8000 rpm for 15 min after 13-14 hr to remove small spherical particles. After discarding the supernatant, 0.02 M of CTAB was used for resuspension of the residue and stored at room temperature for carrying out further experiments.

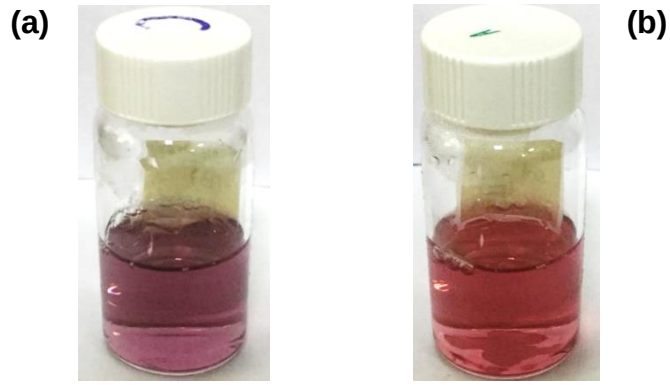

Fig 3.4.2: Gold nanorods synthesized by seed mediated growth mechanism by seed-mediated growth mechanism (a) GNR (B) (b) GNR (E).

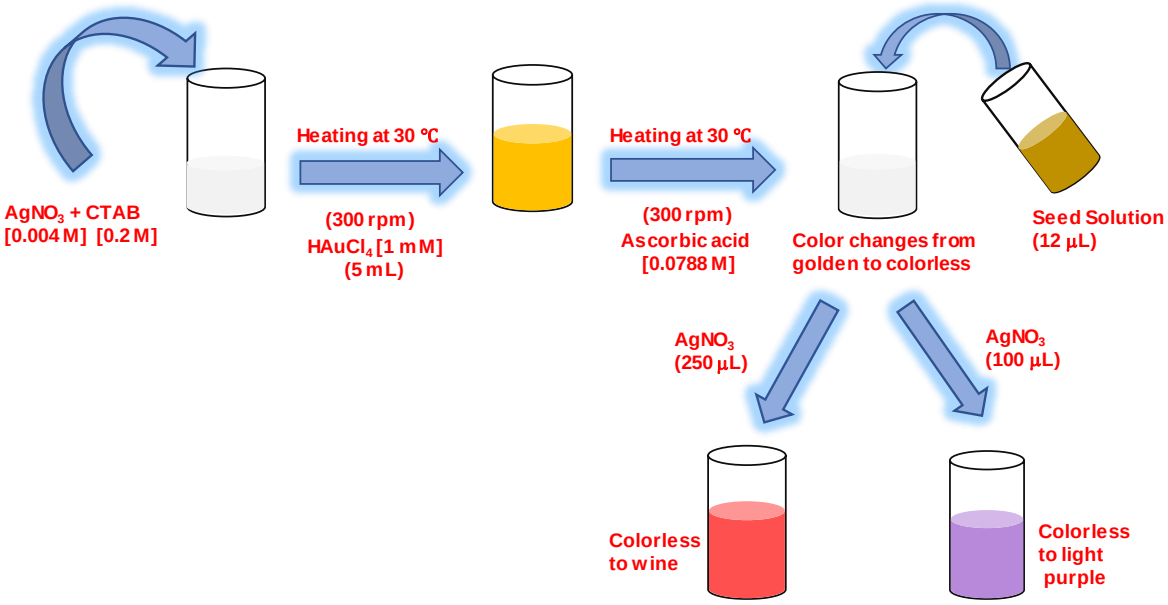

Fig 3.4.3: Schematic diagram for the synthesis of GNR growth solution.

3.5 GNRs based sensor for heavy metal ions detection

The experiments on GNRs-based for heavy metal ions sensing Cr (VI) and Hg(II)) were carried out using a reported literature procedure Li *et al.* (2011) [8]. Typically, 1 mL of GNRs were taken in a 20 mL glass vial, and to it 1 mL of HCl (0.5 M) was added. Then 1 mL of metal ion solution of different concentration (0.5-20 µM) was added. After the proper mixing of the

solutions, they were incubated for 30 min at 50 ℃, following which the solutions were kept on ice for 2 min to cool down prior to UV-Vis measurements.

3.5.1 Sensitivity of heavy metal ion detection by GNRs

For the sensitivity experiment, 1 mL of GNRs were taken in the 20 mL of glass vial and to it 1 mL of HCl (0.5 M) was added. Then 1 mL of metal ion solution of different concentration (20×10^{-4} M to 20×10^{-8} M) was added. After the proper mixing of the solutions, they were incubated for 30 min at 50 ℃, following which the solutions were kept on ice for 2 min to cool down prior to UV-Vis measurements.

3.5.2 GNRs based heavy metal ion sensing at variable incubation times

This experiment was carried out for only Cr (VI) (20 μM) metal ion. In this experiment, 1 mL of GNRs were taken in the 20 mL of glass vial and to it 1 mL of HCl (0.5 M) was added. Then 1 mL Cr (VI) (20 μM) metal ion was added. After the proper mixing of the solutions, they were incubated for different time durations (0 min, 15 min, 30 min, 45 min, 60 min, 90 min, 120 min) at 50 ℃, following which the solutions were kept on ice for 2 min to cool down prior to UV-Vis measurements.

3.5.3 GNRs prepared by variable concentration of CTAB for heavy metal ion sensing

In this experiment, different GNRs were prepared with 5 different CTAB concentration (0.02 M, 0.04 M, 0.06 M, 0.08 M, 0.1 M). 1 mL of GNRs were taken in the 20 mL of glass vial and to it 1 mL of HCl (0.5 M) was added. Then 1 mL of metal ion solution of different concentration (10 μM, 20 μM) was added. After the proper mixing of the solutions, they were incubated for 30 min at 50 ℃, following which the solutions were kept on ice for 2 min to cool down prior to UV-Vis measurements.

4.1 Characterization of gold nanorod and their interaction with heavy metal ions by using UV-Visible absorption Spectroscopy

For the characterisation of synthesized gold nanorods (GNRs) as well as for studying the nanorods-heavy metal ions interactions, UV-Vis Spectroscopy was used extensively. The scan range was 400 nm - 1100 nm for all the collected spectra at the room temperature (See Materials and Methods). The heavy metal ions selected for the gold nanorod interaction were Cr(VI) and Hg(II).

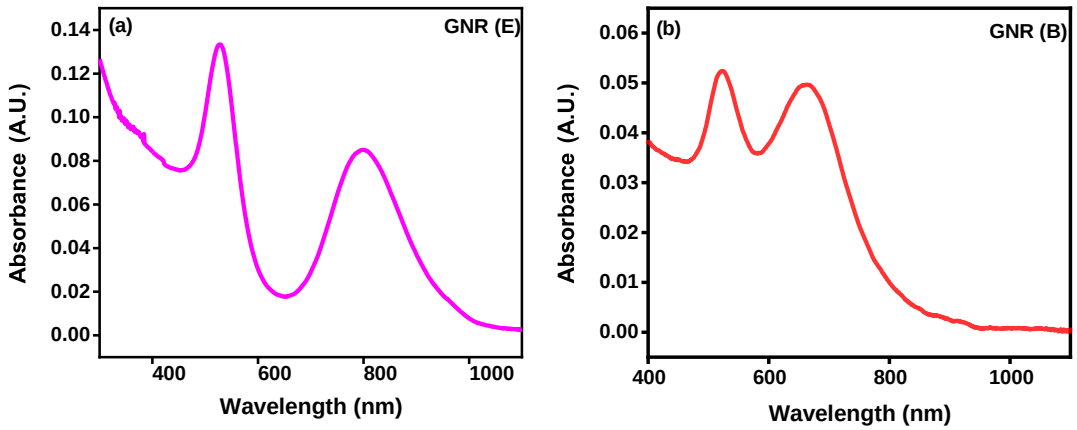

Fig. 4.1. UV-Vis absorption spectra of CTAB-capped gold nanorods (a) GNR (E) (b) GNR (B).

The gold nanorods were synthesized according to a reported protocol (details are mentioned in Chapter 3 of this thesis) and their absorbance was characterized using UV-Vis spectroscopy. It was observed that the aspect ratio of the gold nanorod increases with enhancing the silver ion volume in the growth solution which agrees well with previous reports [El-Sayed Chem Mater 2003]. For instance, in GNR (E) (fig. 4.1a), the longitudinal plasmon band was observed at 799 nm with the volume of $AgNO_3$ (250 μL) at the concentration of 0.004 M, whereas in the GNR (B) (fig. 4.1b), the longitudinal plasmon band was observed at 663 nm with the volume of $AgNO_3$ (100 μL) at the concentration of 0.004 M. Following the characterization of gold nanorods of two different aspect ratios, investigation on effects of size of these nanorods on sensing of heavy metal ions viz. Cr (VI) and Hg (II) were carried out. There were two SPR peaks observed at 525 nm and 799

nm in the initial GNR (E), corresponding to transverse surface plasmon resonance absorption (TPA) and longitudinal plasmon absorption (LPA). However, as per previous reports, the changes in longitudinal surface plasmon resonance (LSPR) absorption of GNR (E) was monitored. It was observed that the longitudinal plasmon band at 799 nm, showed decrease in the wavelength as well as a drop in the absorbance as the concentration of Cr (VI) enhanced from (0.5 M - 20 M) (fig. 4.2a). The progressive blue-shift in LSPR as a function of an increasing Cr (VI) concentration was attributed to the decrease in the aspect ratio (length/width) of GNRs as a result of etching of GNRs by Cr (VI). The etching was attributed to the following: It is well known that the electron potential of Au (I)/Au (0) is 1.691 eV. The Br^- ion and Cl^- ion of CTAB and HCl act as a ligands of gold, the electron potential of Au (I)/Au (0) decreases. Cr (VI) enables to oxidize GNRs, as the standard electron potential of Cr (VI) (1.33 eV) is higher than that of Au (I)/Au (0) in the presence of Br^- and Cl^- ions. Hence, notable decrease in the length of GNR (E) was observed due to the redox etching activated by Cr (VI). However, upon addition of Hg (II) metal ion, the longitudinal plasmon absorption of GNR (E) remained constant even with an increase in the concentration of Hg (II) as shown in (fig. 4.2b).

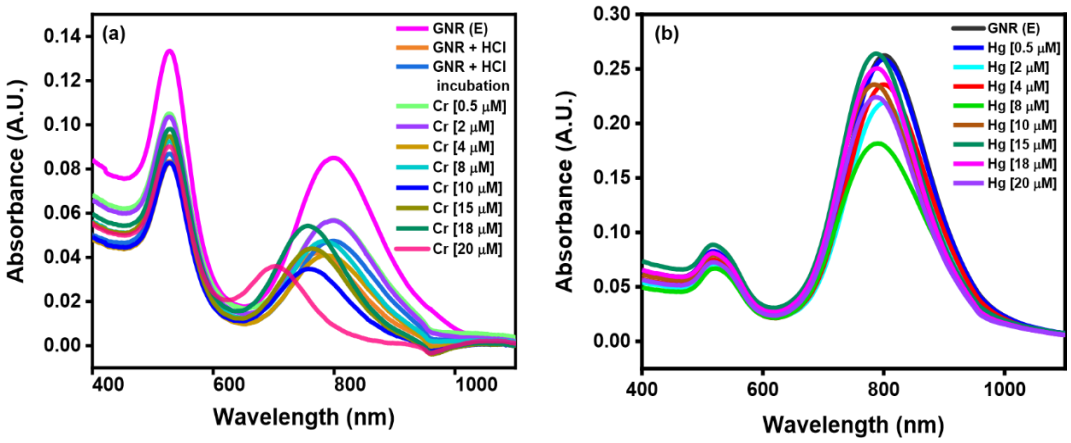

Fig. 4.2. UV-Visible absorption spectra of effect of heavy metal ions on GNR (E) (a) Conc. dependent study of Cr (VI) at 50 °C for 30 min (b) Conc. dependent study of Hg (II) at 50 °C for 30 min.

Next, in order to estimate the sensitivity of the GNR E regarding sensing of heavy metal ions, the concentrations of the analytes were varied in orders of magnitude i.e. from 20×10^{-4} M - 20×10^{-8} M. With an increase in the concentration of Cr (VI) from 10^{-8} – 10^{-5} M, the longitudinal plasmon absorption decreased progressively with a concomitant blue-shift as expected (fig. 4.3c). However, at a high concentration of Cr (VI) (2×10^{-4} M), the longitudinal plasmon band completely invisible and a strong absorbance at 356 nm was observed. We propose that the apparent disappearance of the LSPR band could be due to an excessive etching of GNR (E) by the respective metal ion (fig. 4.3a).

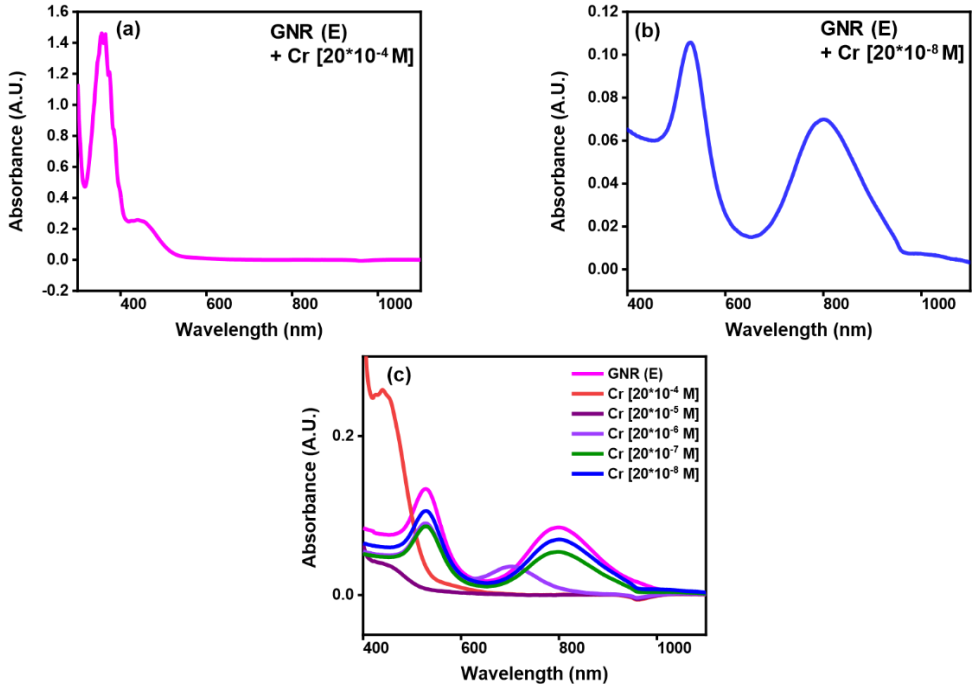

Fig. 4.3. UV-Visible absorption spectra of effect of heavy metal ions on GNR (E) for Cr (VI) at 50 °C for 30 min (a) Sensitivity dependent study of Cr (VI) [2×10^{-4} M] (b) Sensitivity dependent study of Cr (VI) [2×10^{-8} M] (c) Sensitivity dependent study of Cr (VI) from [2×10^{-4} M]- [2×10^{-8} M].

Similar studies were carried out for GNR (B) which have a lower aspect ratio than GNR (E). It was observed that with an increase in the concentration Cr (VI) and Hg (II), there is no gradual decrease in the longitudinal plasmon absorption as shown in (figs. 4.4 & 4.5).

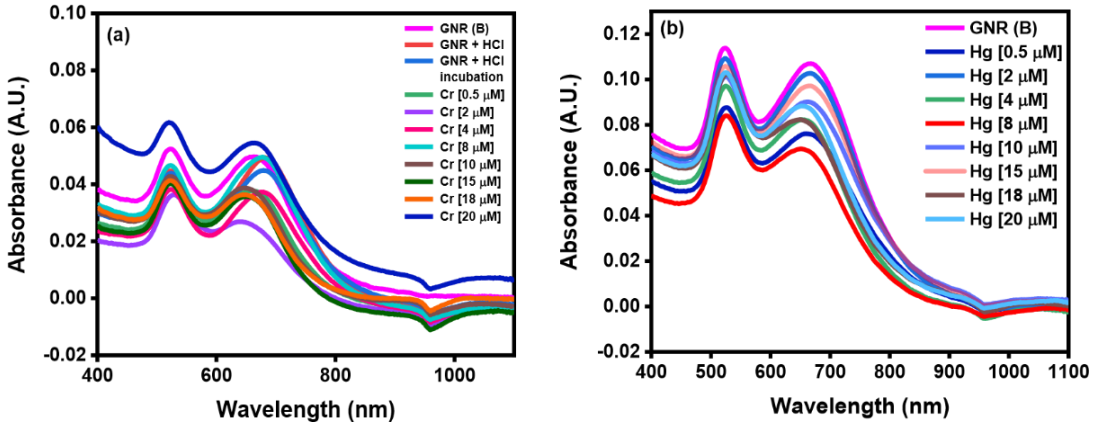

Fig. 4.4. UV-Visible absorption spectra of effect of heavy metal ions on GNR (B) (a) Conc. dependent study of Cr (Ⅵ) at 50 ℃ for 30 min (b) Conc. dependent study of Hg (Ⅱ) at 50 ℃ for 30 min.

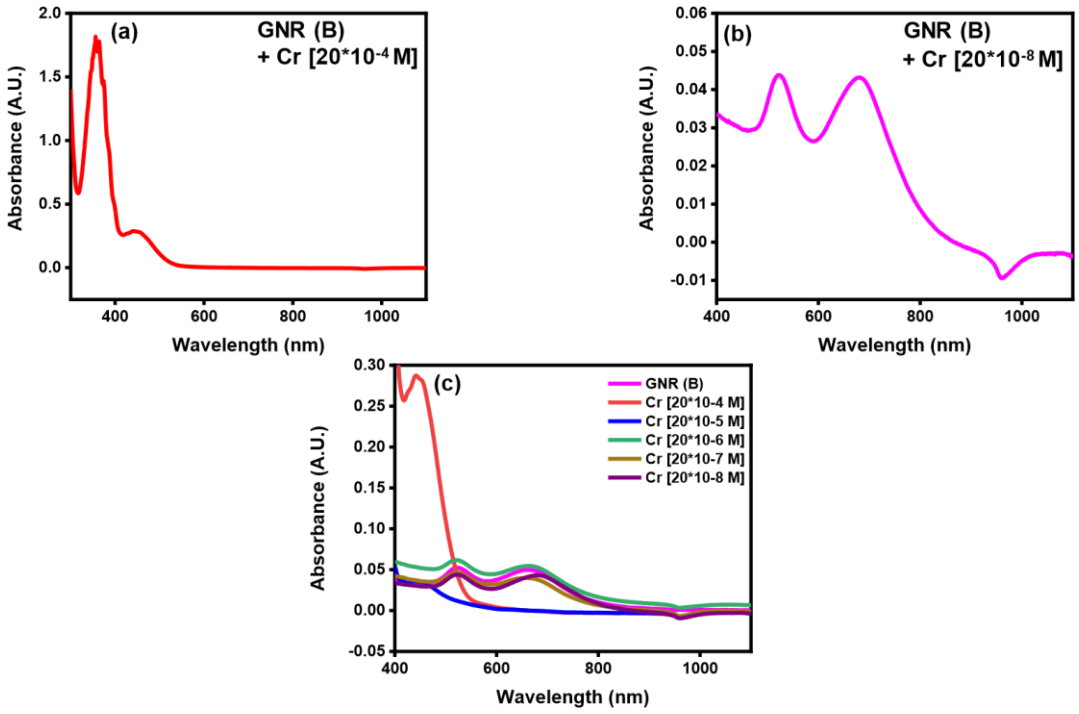

Fig. 4.5. UV-Visible absorption spectra of effect of heavy metal ions on GNR (B) for Cr (VI) at 50 °C for 30 min (a) Sensitivity dependent study of Cr (VI) [2×10^{-4} M] (b) Sensitivity dependent study of Cr (VI) [2×10^{-8} M] (c) Sensitivity dependent study of Cr (VI) from [2×10^{-4} M]- [2×10^{-8} M].

As mentioned in Chapter 3 of this thesis, the GNRs and heavy metal ions were incubated at 50 °C for 30 min following which they were characterized using UV-Vis spectroscopy. Next, in order to assess whether the duration of incubation has any impact on etching of GNRs by metal ions, all the reactions were carried out by incubating the samples at 50 ℃ with a constant concentration of Cr (VI) at 20 μM and varied time from (0 min – 120 min). It was observed that the selective etching is indeed time-dependent. The aspect ratios (length/width) of both the GNRs (E) and (B) gradually decreased as a function of the incubation period whereby the decrease for GNR (E) was more prominent than GNR (B) which indicated that the etching of Cr (VI) is enhanced for the former compared to the latter nanorods (fig. 4.6).

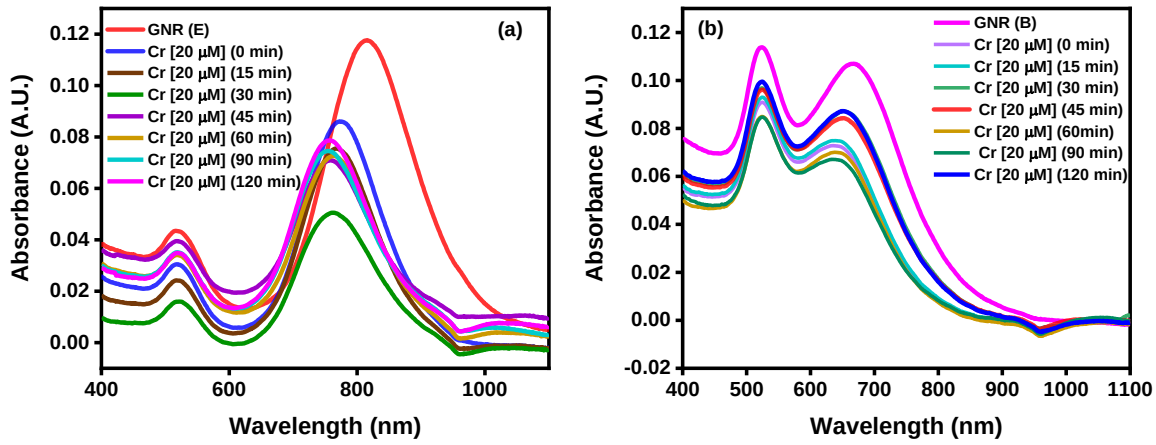

Fig. 4.6. UV-Visible absorption spectra of effect of heavy metal ion Cr (VI) [20 μM] (a) Time dependent study for GNR (E) at 50 °C (b) Time dependent study for GNR (B) at 50 °C.

Next, the effect of concentration of CTAB on heavy metal-induced etching of GNRs was investigated because it is proposed that an increase in CTAB concentration on the GNR surface will significantly reduce/forbid etching. For this set of experiments, the concentration of CTAB was varied from 0.02 M to 0.1 M. We observed that the longitudinal plasmon absorption increased with an increase in CTAB concentration as shown in (fig. 4.7). However upon addition of Cr (VI) [10 μM and 20 μM] in the GNR (E) solution, we found that the etching process of the GNRs enhanced significantly (fig. 4.8) with an increase in the concentration of CTAB which is in contrary to the proposed hypothesis. It was proposed that the amount of bromide ions increases as the CTAB

concentration is increased. Consequently, the electron potential of gold is reduced which in turn increases the response of GNRs as sensor towards Cr (VI).

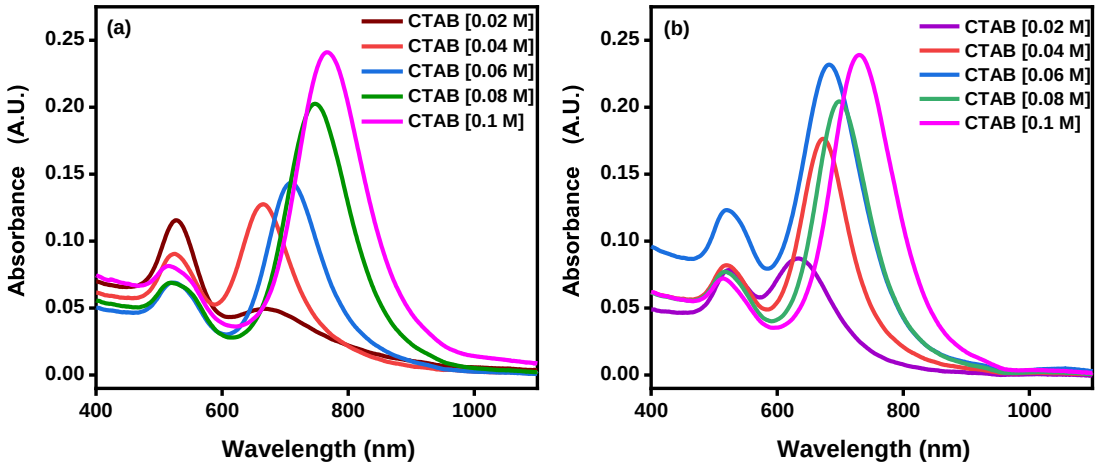

Fig. 4.7. UV-Visible absorption spectra of CTAB conc. dependent study (a) For GNR (E) at 50 °C for 30min (b) For GNR (B) at 50 °C for 30min.

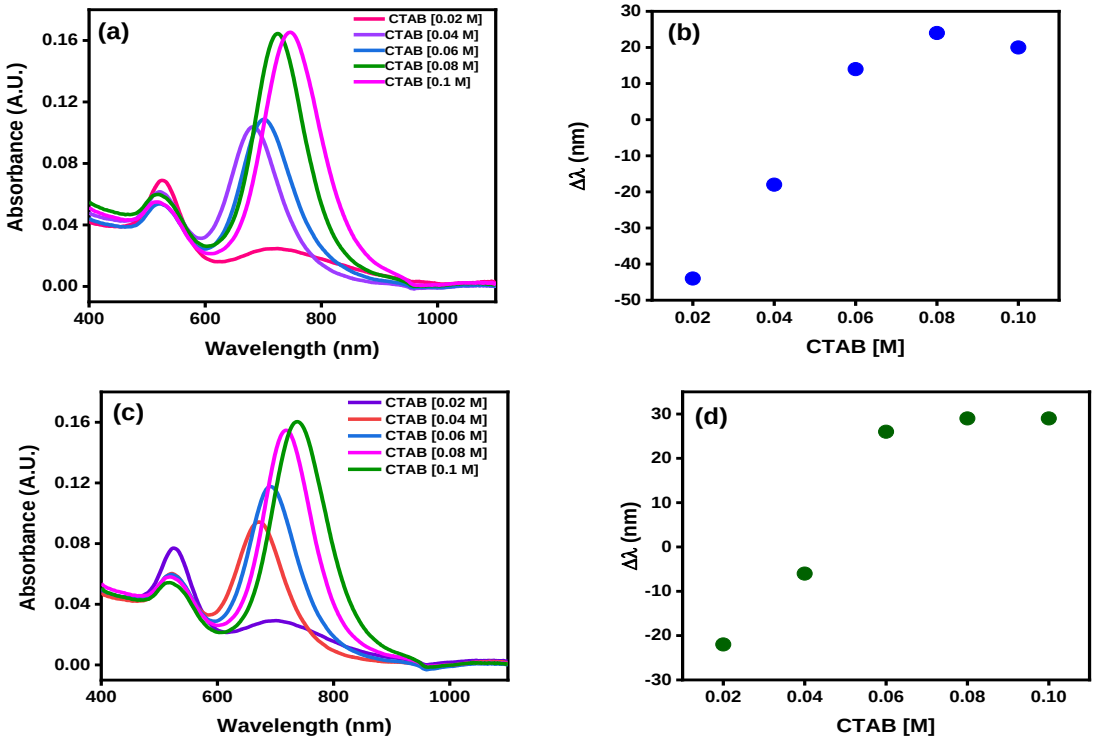

Fig. 4.8. UV-Visible absorption spectra of effect of heavy metal ion Cr (VI) at 50 °C for 30 min (a) CTAB conc. dependent study of Cr (VI) [10 μM] on GNR (E) (b) Effect of CTAB conc. on the Δλ of Cr (VI) [10 μM] on GNR (E) (c) CTAB conc. dependent study of Cr (VI) [20 μM] on GNR (E) (d) Effect of CTAB conc. on the Δλ of Cr (VI) [20 μM] on GNR (E).

A similar trend was observed upon addition of Hg (II) to GNR (E) (fig. 4.9).

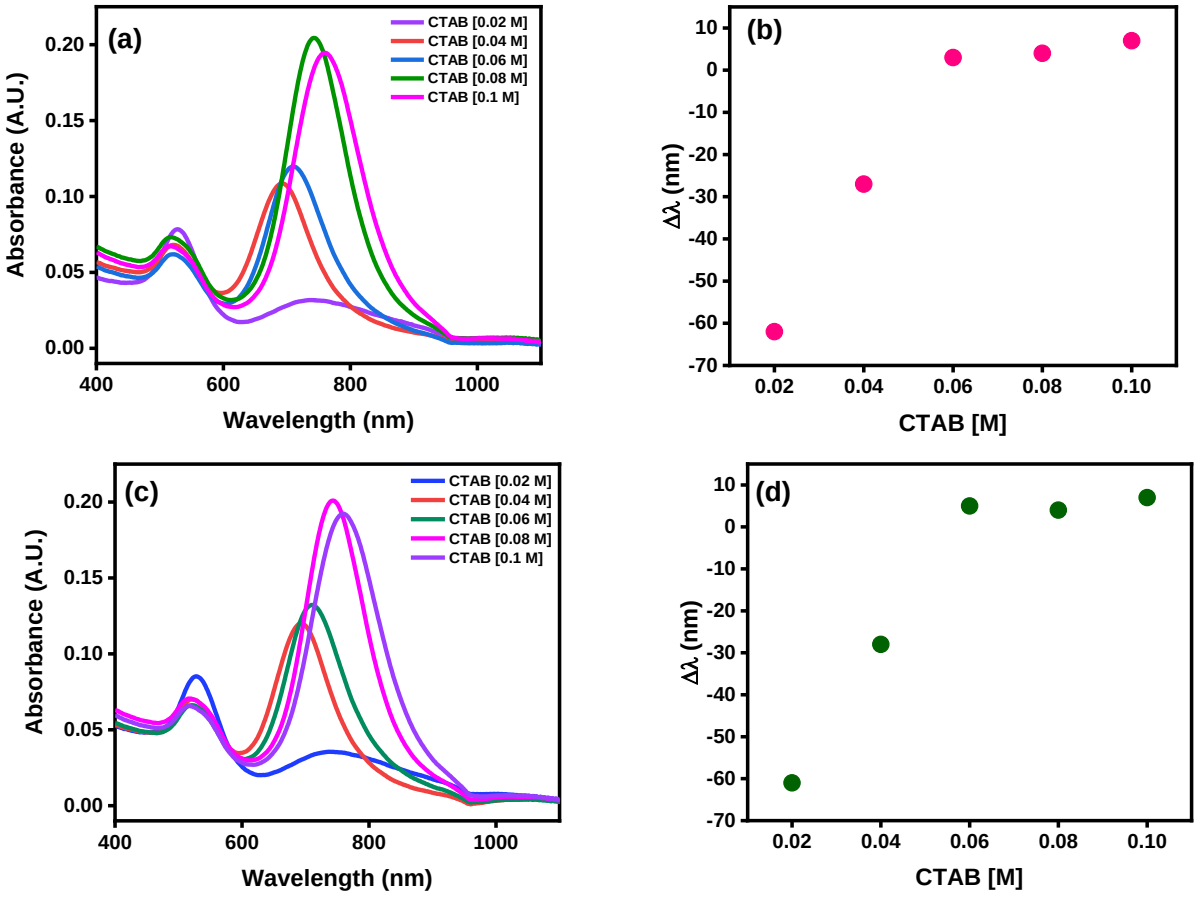

Fig. 4.9. UV-Visible absorption spectra of effect of heavy metal ion Hg (II) at 50 °C for 30 min (a) CTAB conc. dependent study of Hg [10 μM] on GNR (E) (b) Effect of CTAB conc. on the Δλ of Hg [10 μM] on GNR (E) (c) CTAB conc. dependent study of Hg [20 μM] on GNR (E) (d) Effect of CTAB conc. on the Δλ of Hg [20 μM] on GNR (E).

Next, in order to probe the effect of etching of GNR (B) as a function of CTAB concentration, similar studies were carried out using Cr (VI) and Hg (II). As expected, a similar trend was observed as that of GNR (E) (figs. 4.10, 4.11).

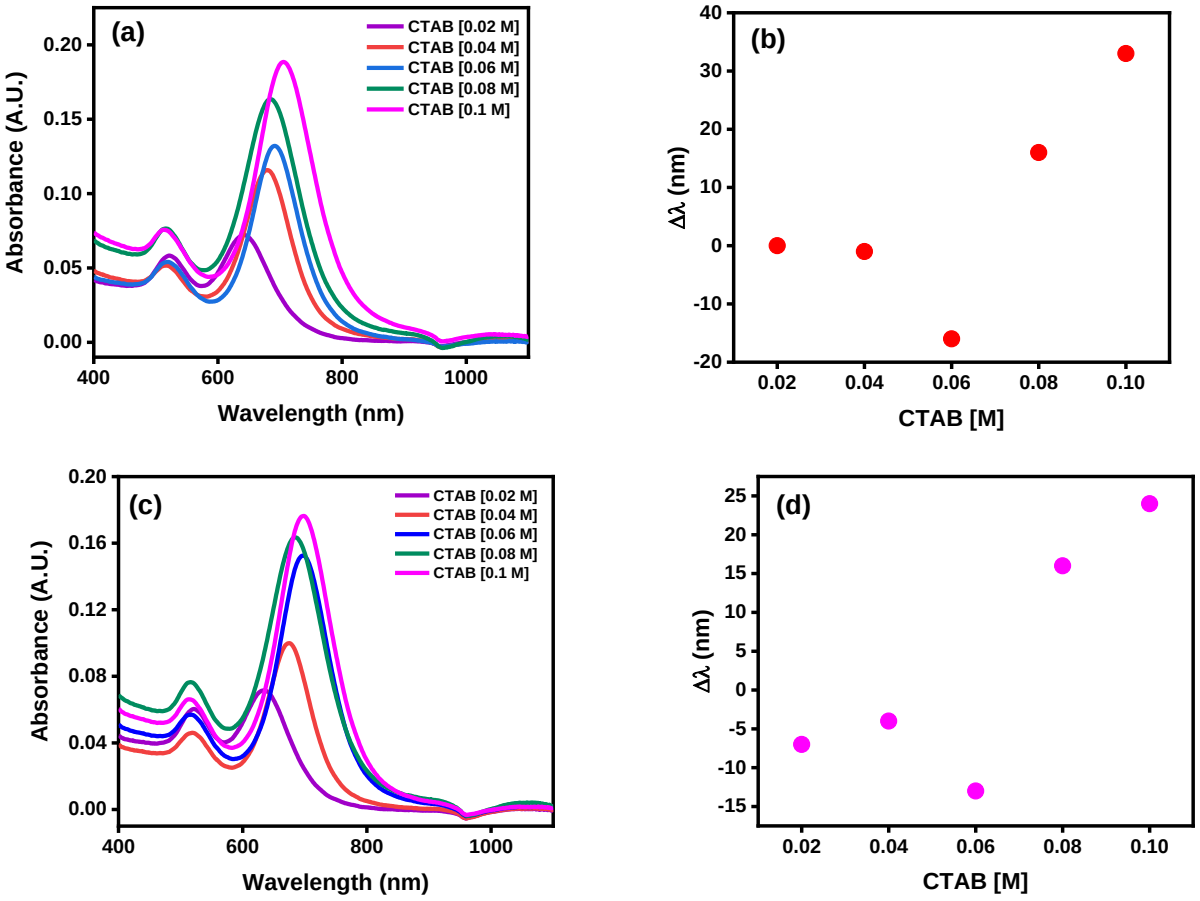

Fig. 4.10. UV-Visible absorption spectra of effect of heavy metal ion Cr (VI) at 50 °C for 30 min (a) CTAB conc. dependent study of Cr [10 μM] on GNR (B) (b) Effect of CTAB conc. on the Δλ of Cr [10 μM] on GNR (B) (c) CTAB conc. dependent study of Cr [20 μM] on GNR (B) (d) Effect of CTAB conc. on the Δλof Cr [20 μM] on GNR (B).

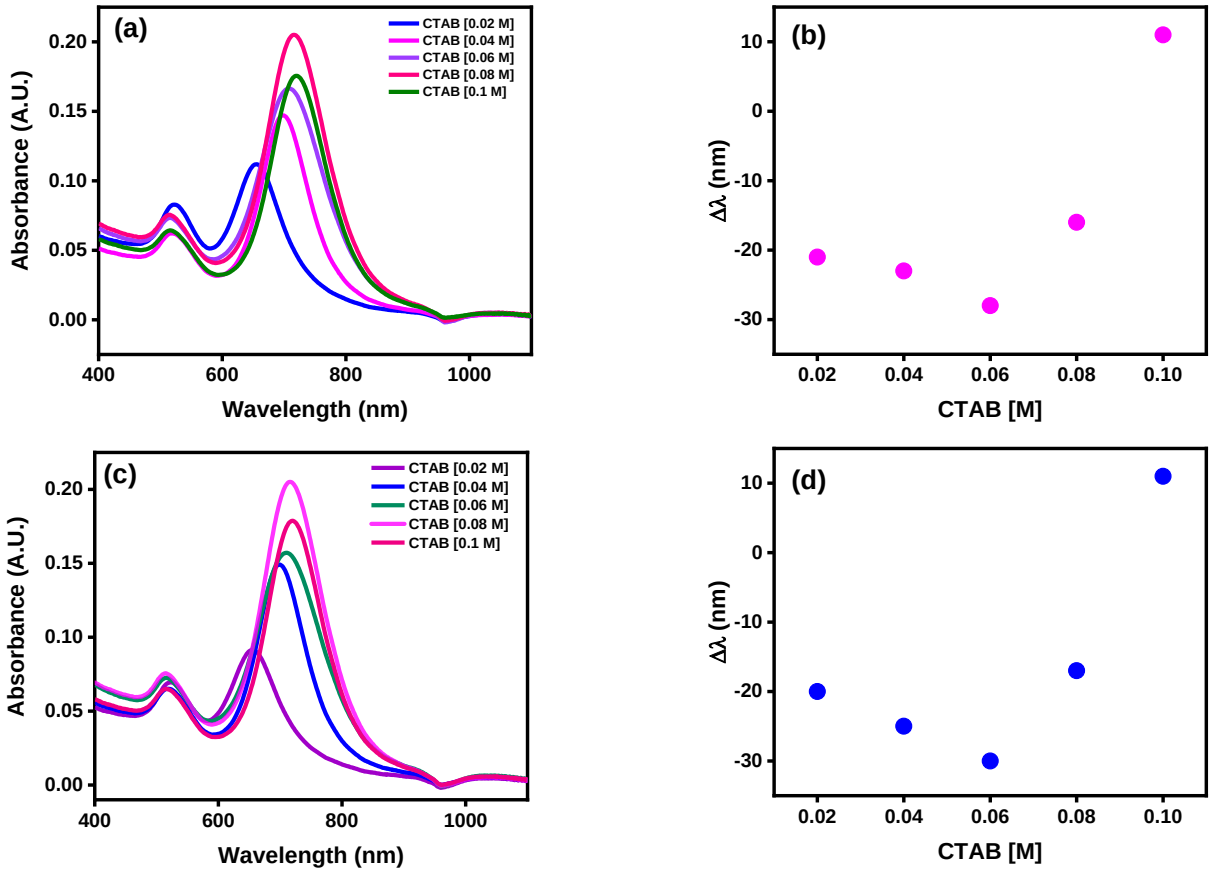

Fig. 4.11. UV-Visible absorption spectra of effect of heavy metal ion Hg (II) at 50 °C for 30 min (a) CTAB conc. dependent study of Hg [10 μM] on GNR (B) (b) Effect of CTAB conc. on the Δλ of Hg [10 μM] on GNR (B) (c) CTAB conc. dependent study of Hg [20 μM] on GNR (B) (d) Effect of CTAB conc. on the Δλ of Hg [20 μM] on GNR (B).

Fig 4.12. TEM image for GNR (E) + 20 μM of Cr (VI) after 5 days

Transmission electron microscopy (TEM) of CTAB capped GNR (E) in the presence of 20 μM Cr (VI) further confirmed that the aspect ratio of GNR (E) decreases due to the redox etching induced by the Cr (VI).

CHAPTER 5 CONCLUSIONS

The present study illustrates our investigation on interaction of heavy metal ions with gold nanorods. Two different sizes of gold nanorods namely, GNR (B) and GNR (E) with different aspect ratios, were synthesized in this study by seed mediated growth mechanism and the nanorods were characterized by UV-Vis spectroscopy extensively. We have observed that for GNR (E), the longitudinal plasmon resonance band appears at a longer wavelength compared to that of GNR (B) since silver deposition on the facet [110] is enhanced than that of the end facet [100] of the gold nanorods which enhances the aspect ratio (length/width). Additionally, the shift in the longitudinal surface plasmon resonance (LSPR) band was observed due to the changes in the concentration of cetyltrimethylammonium bromide (CTAB), variable concentration of heavy metal ions, and variable concentration of silver ions. Our findings revealed that the length of gold nanorods shorten significantly due to the redox etching of gold nanorods by Cr (VI) compared to that of Hg (II) and the effect was more prominent for longer GNR(E) compared to the shorter GNR(B). A linear relationship is shown by the blue shift of longitudinal surface plasmon resonance absorption (LSPA) with concentration of Cr (VI).

CHAPTER 6 REFERENCES

1. Das, M.; Shim, K. H.; An, S. H. A.; Yi, D. K. Review on gold nanoparticles and their applications *Toxical. Environ. Health Sci.* **2011**, *3*, 193-205.
2. Khan, A. K.; Rashid, R.; Murtaza, G.; Zahra, A. Gold nanoparticles synthesis and applications in drug delivery. *Trop J Pharm Res* **2014**, *13*, 1169-1177.
3. Cheng, W.; Dong, S.; Wang, E. Synthesis and self-assembly of cetyltrimethylammonium bromide capped gold nanoparticles. *Langmuir* **2003**, *19*, 9434-9439.
4. Esumi, K.; Matsuhisa, K.; Torigoe, K. Preparation of rodlike gold particles by UV irradiation using cationic micelles as a template. *Langmuir* **1995**, *11*, 3285-3287.
5. Murphy, C. J.; Sau, T. K.; Gole, A. M.; Orendorff, C. J.; Gao, J.; Gou, L.; Hunyadi, S. E.; Li, T. Anisotropic metal nanoparticles synthesis, assembly and optical applications. *J. Phys. Chem B.* **2005**, *109*, 13857-13870.
6. Rao, H.; Xue, X.; Wang, H.; Xue, Z. Gold nanorod etching-based multicolorimetric sensors strategies and applications. *J. Mater. Chem. C* **2019**, *7*, 4610-4621.
7. Huang, X.; El-Sayed, I. H.; Qian, W.; El-Sayed, M. A. Cancer cell imaging and photothermal therapy in the near infrared region by using gold nanorods. *J. Am. Chem. Soc.* **2006**, *128*, 2115-2120.
8. Ding, H.; Yong, K. T.; Roy, I.; Pudavar, H. E.; Law, W. C.; Bergey, E. J.; Prasad, P. N. Gold nanorods coated with multilayer polyelectrolyte as contrast agents for multimodal imaging. *J. Phys. Chem. C* **2007**, *111*, 12552-12556.
9. Li, F. M.; Liu, J. M.; Wang, X. X.; Lin, L. P.; Cai, W. L.; Lin, X.; Zeng, Y. N.; Li, Z. M.; Lin, S. Q. Non-aggregation based label colorimetric sensor for the detection of Cr (VI) based on selective etching of gold nanorods. *Sensors and Actuators B* **2011**, *155*, 817-822.
10. Zhang, X.; Liu, W.; Li, X.; Zhang, Z.; Shan, D.; Xia, H.; Zhang, S.; Lu, X. Ultrahigh selective colorimetric quantification of Chromium (VI) ions based on gold amalgam catalyst oxidoreductase-like activity in water. *Anal. Chem* **2018**, *90*, 4309−14315.
11. Nikoobakht, B.; El-Sayed, M. A. Preparation and growth mechanism of gold nanorods (NRs) using seed-mediated growth method. *Chem. Mater* **2003**, *15*, 1957-1962.
12. Vigderman, L.; Khanal, B. P.; Zubarev, E. R. Functional gold nanorods synthesis, self-assembly and sensing applications. *Adv. Mater* **2012**, *24*, 4811-4841.

13. Haes, A. J.; Stuart, D. A.; Nie, S.; Van Duyne, R. P. Using solution-phase nanoparticles, surface-confined nanoparticle arrays and single nanoparticles as biological sensing platforms. *J. Fluoresc* **2004**, 14, 355-367.
14. Zou, R. X.; Guo, X.; Yang, J.; Li, D. D.; Peng, F.; Zhang, L.; Wang, H. J.; Yu, H. Selective etching of gold nanoparticle by ferric chloride at room temperature. *Cryst. Eng. Commun.* **2009**, *11*, 2797-2803.
15. Gole, A.; Murphy, C. J. Seed-mediated synthesis of gold nanorods role of the size and nature of the seed. *Chem. Mater* **2004**, *16*, 3633-3640.
16. Orendorff, C. J.; Murphy, C. J. Quantitation of metal content in the silver-assisted growth of gold nanorods. *J. Phys. Chem. B* **2006**, *110*, 3990-3994.
17. Cheng, X.; Huang, Y.; Yuan, C.; Dai, K.; Jiang, H.; Ma, J. Colorimetric detection of α-glucosidase activity based on the etching of gold nanorods and its applications to screen anti-diabetic drugs. *Sensors and actuators. B. Chemical* **2019**, *282*, 838-843.
18. Huang, X.; Neretina, S.; El-Sayed, M. A. Gold nanorods from synthesis and properties to biological and biomedical applications. *Adv. Mater* **2009**, *21*, 4880-4910.
19. Johnson, C. J.; Dujardin, E.; Davis, S. A.; Murphy, C. J.; Mann, S. Growth and form of gold nanorods prepared by seed-mediated, surfactant-directed synthesis. *J. Mater. Chem* **2002**, *12*, 1765–1770.
20. Zhang, Z.; Chen, Z.; Qu, C.; Chen, L. Highly sensitive visual detection of copper ions based on the shape-dependent LSPR spectroscopy of gold nanorods. *Langmuir* **2014**, *30*, 3625−3630.

T

ORIGINALITY REPORT

15%	3%	11%	6%
SIMILARITY INDEX	INTERNET SOURCES	PUBLICATIONS	STUDENT PAPERS

PRIMARY SOURCES

1	Fei-Ming Li, Jia-Ming Liu, Xin-Xing Wang, Li-Ping Lin, Wen-Lian Cai, Xuan Lin, Yi-Na Zeng, Zhi-Ming Li, Shao-Qin Lin. "Non-aggregation based label free colorimetric sensor for the detection of Cr (VI) based on selective etching of gold nanorods", Sensors and Actuators B: Chemical, 2011 Publication	2%
2	Babak Nikoobakht, Mostafa A. El-Sayed. "Preparation and Growth Mechanism of Gold Nanorods (NRs) Using Seed-Mediated Growth Method", Chemistry of Materials, 2003 Publication	1%
3	Qi Yuan Chen, Jian Bo Xiao, Xiao Qing Chen. "Rapid determination of organic acids in Bayer liquors by high-performance liquid chromatography after solid-phase extraction", Minerals Engineering, 2006 Publication	1%
4	Zhang, Zhiyang, Zhaopeng Chen, Chengli Qu, and Lingxin Chen. "Highly Sensitive Visual	1%

	Detection of Copper Ions Based on the Shape-Dependent LSPR Spectroscopy of Gold Nanorods", Langmuir Publication	
5	Submitted to Middle East Technical University Student Paper	1%
6	Xia Guo, Qiao Zhang, Yanghui Sun, Qing Zhao, Jian Yang. "Lateral Etching of Core–Shell Au@Metal Nanorods to Metal-Tipped Au Nanorods with Improved Catalytic Activity", ACS Nano, 2012 Publication	1%
7	Linzhuang Xing, Bin Chen, Dong Li, Jun Ma, Wenjuan Wu, Guoxiang Wang. "Nd:YAG laser-induced morphology change and photothermal conversion of gold nanorods with potential application in the treatment of port-wine stain", Lasers in Medical Science, 2017 Publication	1%
8	en.wikipedia.org Internet Source	1%
9	Chungang Wang. "Gold Nanorod Probes for the Detection of Multiple Pathogens", Small, 12/2008 Publication	1%
10	Harshala J. Parab, Hao Ming Chen, Nitin C. Bagkar, Ru-Shi Liu, Yeu-Kuang Hwu, Din Ping	<1%

Tsai. "Approaches to the Synthesis and Characterization of Spherical and Anisotropic Noble Metal Nanomaterials", Wiley, 2010
Publication

---

11 Lu, Simin, Ling Chen, Ping Yang, and Katarzyna Matras-Postolek. "Highly sensitive visual detection of catalase based on the accelerating decomposition of H2O2 using Au nanorods as a sensor", RSC Advances, 2016.
Publication <1%

---

12 Submitted to National Institute Of Technology, Tiruchirappalli
Student Paper <1%

---

13 Junwei Xin, Fuqiang Zhang, Yuexia Gao, Yanyan Feng, Shougang Chen, Aiguo Wu. "A rapid colorimetric detection method of trace Cr (VI) based on the redox etching of Agcore–Aushell nanoparticles at room temperature", Talanta, 2012
Publication <1%

---

14 sites.google.com
Internet Source <1%

---

15 Sujin Lee, Yun-Sik Nam, Sung-Hee Choi, Yeonhee Lee, Kang-Bong Lee. "Highly sensitive photometric determination of cyanide based on selective etching of gold nanorods", Microchimica Acta, 2016 <1%

	Publication	
16	Submitted to Université Claude Bernard Lyon 1 Student Paper	<1%
17	Submitted to University of Strathclyde Student Paper	<1%
18	ethesis.nitrkl.ac.in Internet Source	<1%
19	Longhua Tang, Jinghong Li. "Plasmon-Based Colorimetric Nanosensors for Ultrasensitive Molecular Diagnostics", ACS Sensors, 2017 Publication	<1%
20	Submitted to Hofstra University Student Paper	<1%
21	Jia-Ming Liu, Li Jiao, Ma-Lin Cui, Li-Ping Lin, Xin-Xing Wang, Zhi-Yong Zheng, Li-Hong Zhang, Shu-Lian Jiang. "A highly sensitive non-aggregation colorimetric sensor for the determination of I− based on its catalytic effect on Fe3+ etching gold nanorods", Sensors and Actuators B: Chemical, 2013 Publication	<1%
22	Yurong Ma, Yingyi Zhu, Benzhi Liu, Guixiang Quan, Liqiang Cui. "Colorimetric Determination of Hypochlorite Based on the Oxidative Leaching of Gold Nanorods", Materials, 2018 Publication	<1%

23	www.plantphysiol.org Internet Source	<1%
24	dspace.vutbr.cz Internet Source	<1%
25	Submitted to The Hong Kong Polytechnic University Student Paper	<1%
26	Li, F.M.. "Non-aggregation based label free colorimetric sensor for the detection of Cr (VI) based on selective etching of gold nanorods", Sensors & Actuators: B. Chemical, 20110720 Publication	<1%
27	www.goldstreetentertainment.com Internet Source	<1%
28	Submitted to University of Central Florida Student Paper	<1%
29	Liu, Keng-Ku, Sirimuvva Tadepalli, Limei Tian, and Srikanth Singamaneni. "Size-dependent Surface Enhanced Raman Scattering Activity of Plasmonic Nanorattles", Chemistry of Materials Publication	<1%
30	isindexing.com Internet Source	<1%
31	camis.unh.edu Internet Source	<1%

32	Gilles Berhault, Marta Bausach, Laure Bisson, Loïc Becerra, Cécile Thomazeau, Denis Uzio. "Seed-Mediated Synthesis of Pd Nanocrystals: Factors Influencing a Kinetic- or Thermodynamic-Controlled Growth Regime", The Journal of Physical Chemistry C, 2007 Publication	<1%
33	Submitted to University of Wales Institute, Cardiff Student Paper	<1%
34	Perez-Juste, J.. "Gold nanorods: Synthesis, characterization and applications", Coordination Chemistry Reviews, 200509 Publication	<1%
35	research.sabanciuniv.edu Internet Source	<1%
36	Submitted to University of Hong Kong Student Paper	<1%
37	Submitted to Imperial College of Science, Technology and Medicine Student Paper	<1%
38	Submitted to Universiti Teknologi MARA Student Paper	<1%
39	Submitted to University of Sheffield Student Paper	<1%

40 vp-scientific.com
Internet Source

<1%

Exclude quotes	Off	Exclude matches	< 8 words
Exclude bibliography	On		